Oscillations with three damping effects

Xiao-jun Wang[1], Chris Schmitt and Marvin Payne

Department of Physics, Georgia Southern University, Statesboro, GA 30460, USA

E-mail: xwang@gasou.edu

Abstract
Experiments on oscillatory motion are described with three different damping effects. The first experiment is a physical pendulum whose damping mechanism is due to sliding friction; the second is magnetic resistance due to eddy currents; and the third experiment involves a pendulum setup where air resistance is the dominant factor. These three damping mechanisms yield constant ($\vec{v}/|\vec{v}|$), linear, and quadratic resistances in velocity respectively. Approximation methods are described for treating the three damping effects and a general solution is derived for the damping with a very general velocity dependence. A sonic rangefinder is used to record the oscillatory motions of the pendulums. The experimental measurements and theoretical calculations are in a good agreement.

1. Introduction

Oscillatory motions occur throughout nature. For most realistic systems the motions are not simple harmonic but involve damping effects. In this paper, we present experimental setups that demonstrate three different damping effects—constant friction ($\vec{v}/|\vec{v}|$), linear dependence of velocity and quadratic dependence of velocity. The first one demonstrated is the physical pendulum designed so that the damping of the oscillatory motion is due to sliding friction in the support, yielding damped oscillations with the amplitude decreasing linearly with time until the motion abruptly stops. The second experiment uses magnetic eddy currents to slow down a metal pendulum as it moves perpendicular to a magnetic field. A linear damping resistance is then created. The final case involves damping generated by a large sail, where air resistance plays the dominant role, resulting in quadratic damping. Theoretically, the damped effects in the oscillations, including the three cases mentioned above, can be expressed by a dominant damping term that is proportional to v^n, or more precisely, $-|\vec{v}|^{n-1}\vec{v}$, where $\vec{v}$ is the velocity of motion and n an integer. Considering the damping to be small, we derive a general solution for the damping terms with any velocity dependence. Approximation methods are described for treating the damping effects. All the experiments described here are good demonstrations for undergraduate physics majors. Through these experiments students can gain a clear picture

---

[1] Author to whom any correspondence should be addressed.
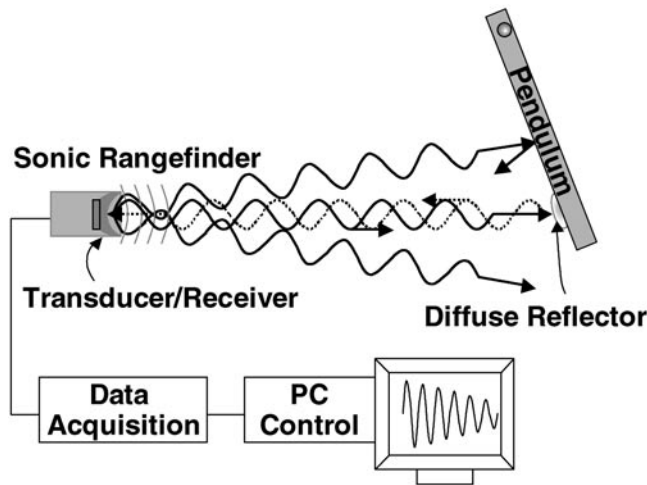
Figure 1. A schematic diagram of the experimental setup. Sound pulses are emitted by the transducer and are collected by the receiver when they are reflected by the diffuse reflector fixed on the moving object. The position of the pendulum as a function of time is recorded and saved to the PC.

of oscillatory motion with different types of friction. They will also learn the principles of the sonic rangefinder, computer data acquisition, A/D conversion, data analysis and computer based nonlinear curve fitting.

2. Experimental

A schematic diagram of the experimental setup is shown in figure 1. A sonic rangefinder (Automate Scientific Inc.) operated at 68 Hz is used to log a detailed record of the position of an object as a function of time. It measures the position by sending out a short collimated pulse of sound in the direction of the object to be studied. The pulse is reflected back to the apparatus by the diffuse reflector fixed on the object and is collected by the receiver. The time that the pulse was sent, t, and the travelling time of the pulse between the rangefinder and the reflector, Δt, are recorded by a computer interfaced with the rangefinder. If V is the speed of sound, the distance, d, of the object from the apparatus is $d = V \Delta t / 2$. To accurately measure the distance, the rangefinder must receive the reflection of the last pulse before sending a new pulse. If we choose the maximum distance to be 2 m, a round trip of the pulse will take 0.012 s ($V = 344$ m s^{-1}), which limits the operating frequency of the rangefinder to be less than 80 Hz. Considering that the average speed of the reflector is $\sim$20 cm s^{-1}, we have a spatial resolution of around 0.2 cm.

3. A general solution

For a one-dimensional oscillation with a damping term proportional to v^n, Newton's second law yields the following differential equation:

$$\frac{\mathrm{d}^2 x}{\mathrm{d}t^2} + \beta \left| \frac{\mathrm{d}x}{\mathrm{d}t} \right|^{n-1} \frac{\mathrm{d}x}{\mathrm{d}t} + \omega x^2 = 0 \tag{1}$$

where β is a non-negative constant depending upon the nature of the friction and geometric parameters of the pendulum and ω is the oscillation frequency. $\mathrm{d}x/\mathrm{d}t$ outside the absolute

value bars indicates that the friction is against the velocity. Since we only deal with the oscillatory motion, the friction should be small so that it causes only small effects over any single oscillation and the angular frequency, ω, changes little compared with ω_0, the frequency without damping. The solution can be expressed by

$$x = A(t)\cos(\omega t + \alpha) \tag{2}$$

where $A(t)$ is the amplitude that is nearly constant over a single oscillation but which slowly decreases over longer periods of time and α is the initial phase. The insensitivity of the frequency of oscillation to small amounts of friction can be demonstrated from the analytical solution to the case which is linear in velocity. This feature persists for the other forms of friction as well. Solution of equation (1) means finding the functional form of $A(t)$ for the different types of friction. We will use the fact that the rate of change of $A(t)$ with respect to time is very small compared with that of the $\cos(\omega t + \alpha)$ term. Correspondingly, the energy, $E(t)$, is nearly conserved over a single oscillation and is given by

$$E(t) = \tfrac{1}{2}M(\omega A(t))^2 \tag{3}$$

or

$$\frac{\mathrm{d}E(t)}{\mathrm{d}t} = M\omega^2 A(t)\frac{\mathrm{d}A(t)}{\mathrm{d}t} \tag{4}$$

where M is the mass of the pendulum. On the other hand, from the work-energy principle, $\mathrm{d}E(t)/\mathrm{d}t$ is also the rate of energy loss due to the frictional force, $\vec{F}_f$, i.e.

$$\frac{\mathrm{d}E(t)}{\mathrm{d}t} = -\vec{F}_f \cdot \vec{v} = -\beta M\left|\frac{\mathrm{d}x}{\mathrm{d}t}\right|^{n+1} \cong -\beta M(\omega A(t))^{n+1}|\sin(\omega t + \alpha)|^{n+1}. \tag{5}$$

From equations (4) and (5) we have,

$$\frac{\mathrm{d}A(t)}{\mathrm{d}t} = -\frac{\beta}{\omega}(\omega A(t))^n |\sin(\omega t + \alpha)|^{n+1}. \tag{6}$$

Since the decrease of the amplitude over a period $T = 2\pi/\omega$, ΔA, is small, we have, approximately

$$\frac{\mathrm{d}A(t)}{\mathrm{d}t} \cong \frac{\Delta A}{T} \tag{7}$$

where

$$\begin{aligned}
\Delta A &\cong \frac{\beta}{\omega}(\omega A(t))^n \int_t^{t+T} |\sin(\omega t + \alpha)|^{n+1}\,\mathrm{d}t \\
&= \frac{4\beta}{\omega^2}(\omega A(t))^n \int_0^{\pi/2} (\sin(u))^{n+1}\,\mathrm{d}u.
\end{aligned} \tag{8}$$

Above we have treated $A(t)$ as a constant when integrating and made use of the periodic properties of the sine function. Finally, we have

$$\frac{\mathrm{d}A}{\mathrm{d}t} = -\frac{2\beta}{\pi}A^n\omega^{n-1}I_n \tag{9}$$

where,

$$I_n = \int_0^{\pi/2} (\sin(u))^{n+1}\,\mathrm{d}u. \tag{10}$$

The cases of interest are $n = 0$, 1 and 2, corresponding to constant, linear and quadratic damping respectively. We will devote sections to the three most important cases together with experimental setups and results. Over the many oscillations that are required for a large decrease in A, equation (9) will give the same accumulated effect as a $\mathrm{d}A/\mathrm{d}t$ that includes the details of the time dependence during each oscillation.
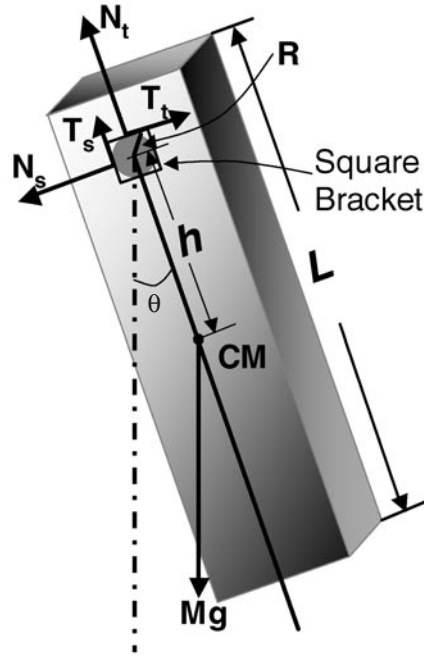
Figure 2. A physical pendulum with constant sliding friction. The forces acting on the pendulum
and the dimensions of the pendulum are illustrated. N and T are the normal and frictional forces
respectively exerted on the brackets by the metal rod through the pendulum. CM: centre of mass.

4. The case $n = 0$: constant sliding friction in a physical pendulum

As shown in figure 2, a pendulum was constructed using a $2'' \times 4''$ wooden board that was
supported by a metallic rod. Sliding friction is created by two square brackets that are attached
to the board and brace the rod.

If the limits for both the coefficient of sliding friction, μ_k, and the initial angular amplitude,
θ_0, are small, i.e. $\mu_k^2 \ll 1$ and $|\theta_0| \ll 1$, we can derive the frictional torque, τ_f, which damps
the motion of the swing board as

$$\tau_f \stackrel{\sim}{=} -\mu_k M g R \, \mathrm{sgn}\left(\frac{\mathrm{d}\theta}{\mathrm{d}t}\right) \tag{11}$$

where M is the mass of the pendulum, g is the gravitational acceleration, R is the radius of the
circular rod, and

$$\mathrm{sgn}\left(\frac{\mathrm{d}\theta}{\mathrm{d}t}\right) = \begin{cases} +1 & \mathrm{d}\theta/\mathrm{d}t > 0 \\ -1 & \mathrm{d}\theta/\mathrm{d}t < 0. \end{cases} \tag{12}$$

Taking the restoring torque, τ_r, equal to $-Mgh\sin\theta \stackrel{\sim}{=} -Mgh\theta$, $I\mathrm{d}^2\theta/\mathrm{d}t^2 = \tau_r + \tau_f$, and
$I = M(h^2 + L^2/12)$ (using the parallel-axis theorem), where h, θ and L are the parameters
shown in figure 2 and I is the moment of inertia of pendulum about the axis of rotation, we
have

$$\frac{\mathrm{d}^2\theta}{\mathrm{d}t^2} + \mu_k\left(\frac{R}{h}\right)\left(\frac{gh}{h^2 + L^2/12}\right)\mathrm{sgn}\left(\frac{\mathrm{d}\theta}{\mathrm{d}t}\right) + \left(\frac{gh}{h^2 + L^2/12}\right)\theta = 0. \tag{13}$$

Comparing this equation with (1), we have, correspondingly, $n = 0$, $\beta = \mu_k R\omega^2/h$, and
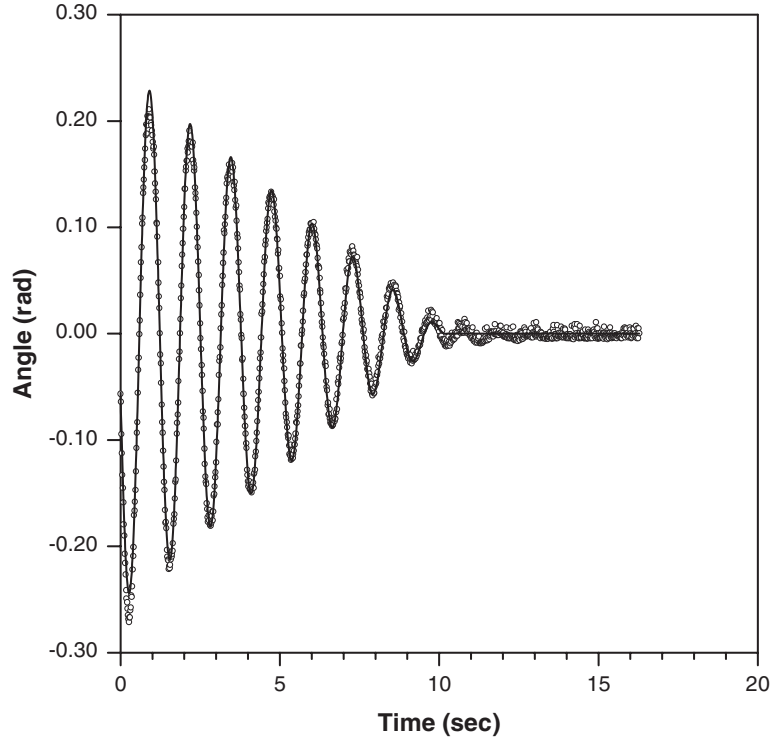
Figure 3. Measured results (circles) as a function of time compared with a curve of best fit (full curve) for the physical pendulum with sliding friction.

$\omega^2 = [gh/(h^2+L^2/12)]$. From equations (9) and (10), we have $I_0 = 1$ and $dA/dt = -2\beta/\pi\omega$. Considering the initial conditions of $\theta(t = 0) = \theta_0$ and $d\theta/dt\big|_{t=0} = 0$, we find

$$A(t) = \theta_0 - \frac{2\mu_k R\omega_0}{\pi h}t \tag{14}$$

or

$$\theta = \left(\theta_0 - \frac{2\mu_k R\omega_0}{\pi h}t\right)\cos(\omega t + \alpha). \tag{15}$$

This equation indicates that the amplitude of the oscillations will decrease linearly with time until the motion abruptly stops ($\tau_f \approx \tau_r$). Figure 3 shows the experimental results (circles) and the theoretical fit (full curve) using equation (15). The values on the y-axis have been converted to angle from the distance recorded directly by the rangefinder by dividing the separation from the axis of rotation down to the diffuse reflector. The linear decrease in the amplitude is clearly observed. The values of the four parameters obtained from the fitting are: $\theta_0 = 0.25$, $2\mu_k R\omega/\pi h = 0.024$ s^{-1}, $\omega = 4.92$ s and $\alpha = 1.79$. The coefficient of sliding friction is then estimated to have a value of 0.3, which is very reasonable [1].

5. The case $n = 1$: linear resistance due to eddy currents

Figure 4 depicts the setup and dimensions of a magnetically damped pendulum. The damping is dominated by the frictional forces due to eddy currents flowing in the aluminium plate when it is allowed to move perpendicular to a magnetic field. The field is generated by the two
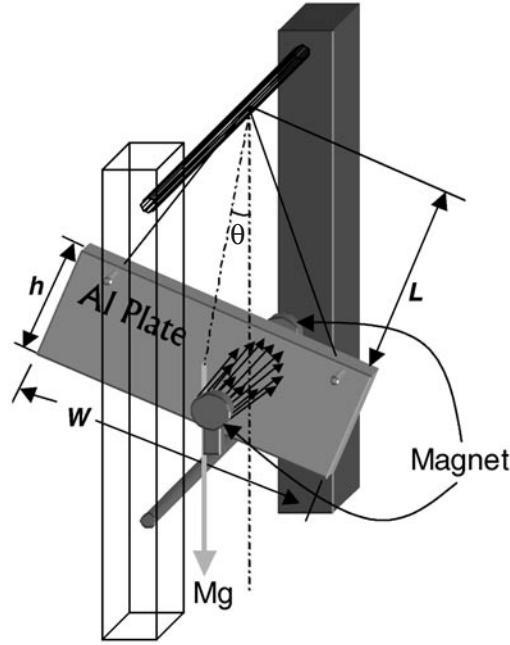
Figure 4. The setup and dimensions of a magnetically damped pendulum. The field is generated by the two round magnets placed one on each side of the conducting plate. The damping is dominated by the frictional forces due to eddy currents flowing in the aluminium plate when it is allowed to move perpendicular to the magnetic field. A diffuse reflector is fixed on one side perpendicular to the plate to provide the return sound pulse.

magnets placed one on each side of the conducting plate. The moment of inertia of the system (using parallel-axis theorem and neglecting the mass of the wires) and the restoring torque can be readily written as

$$I = M(L + h/2)^2 + \frac{M}{12}(h^2 + W^2) \tag{16}$$

$$\tau_R \cong -Mg(L + h/2)\sin\theta \tag{17}$$

where M is the mass of the plate and L, H and W are the dimensions of the pendulum, as shown in figure 4. To find the frictional torque we need to consider the following: when a conductor moves through a magnetic field, $\vec{B}$, a current density is induced which is given by $\vec{J} = \sigma(\vec{F}/q) = \sigma(\vec{v} \times \vec{B})$, where σ is the conductivity of the plate, $\vec{F}/q$ the force per unit charge (electric field) and $\vec{v}$ the velocity of the pendulum. The induced current density has a force on it due to the magnetic field. The force per unit volume is $d\vec{F}/du = \vec{J} \times \vec{B} = -\sigma B^2 \vec{v}$. Integrating over the volume where the magnetic field is non-zero, we find $\vec{F} \cong -\sigma u_{eff} B^2 \vec{v}$, where u_{eff} is the effective volume of the magnetic field in the conducting material. This result is approximate due to the fact that the boundary conditions are not taken into account. The frictional torque is then given by

$$\tau_f \cong -\sigma u_{eff} B^2 (L + h/2)v \cong -\sigma u_{eff} B^2 (L + h/2)^2 \frac{d\theta}{dt}. \tag{18}$$

Again, from $I d^2\theta/dt^2 = \tau_r + \tau_f$, we have

$$\frac{d^2\theta}{dt^2} + \sigma u_{eff} B^2 (L + h/2)^2 \frac{1}{I}\frac{d\theta}{dt} + Mg(L + h/2)\frac{1}{I}\theta = 0. \tag{19}$$
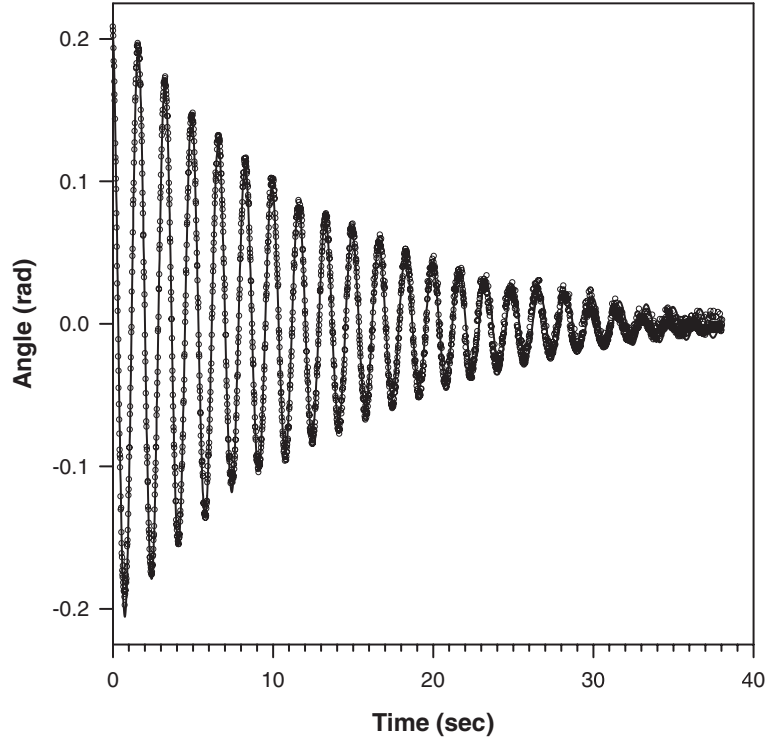
Figure 5. Measured results (circles) as a function of time compared with a curve fit (full curve) with a magnetically damped pendulum.

Comparing this equation with (1), we have, correspondingly, $n = 1$, $\beta = \sigma u_{eff} B^2 (L + h/2)^2 I^{-1}$, and $\omega^2 = Mg(L + h/2)I^{-1}$. From the general solution of equations (9) and (10), we have $I_n = \pi/4$, $A = x_0 e^{-\beta t/2}$ and finally,

$$\theta = \theta_0 e^{-\beta t/2} \cos(\omega t + \alpha). \tag{20}$$

Equation (20) agrees with the exact solution of the original differential equation (1) [2], indicating that the approximation is appropriate provided that the damping during a single period is very small, i.e., $\beta\pi/\omega \ll 1$. Figure 5 shows the experimental results (circles) and theoretical prediction (full curves). The amplitude decreases exponentially as time goes on. The fitting gives the parameters $\beta/2 = 0.08$ s^{-1} and $\omega = 3.76$ s^{-1}, giving $\beta\pi/\omega = 0.067 \ll 1$, which is consistent with our approximation. From the exact solution we also have $\omega = \sqrt{\omega_0^2 - (\beta/2)^2}$. Since β is very small, the difference between ω and ω_0 is calculated to be less than 0.025%, which is negligible. The approximation discussed in section 3, $\omega \approx \omega_0$, holds very well.

6. The case $n = 2$: quadratic resistance due to air friction

Here we consider a pendulum with two strips and a large sail at the bottom, as shown in figure 6. If we call the total mass of the pendulum M, then the mass of two suspending strips of width W_1 and length R is $m_1 = 2M(W_1 R)/S$, where S is the total area of the pendulum. The mass of the large bottom part, the sail with width W and height h, is $m_2 = M(Wh)/S$.
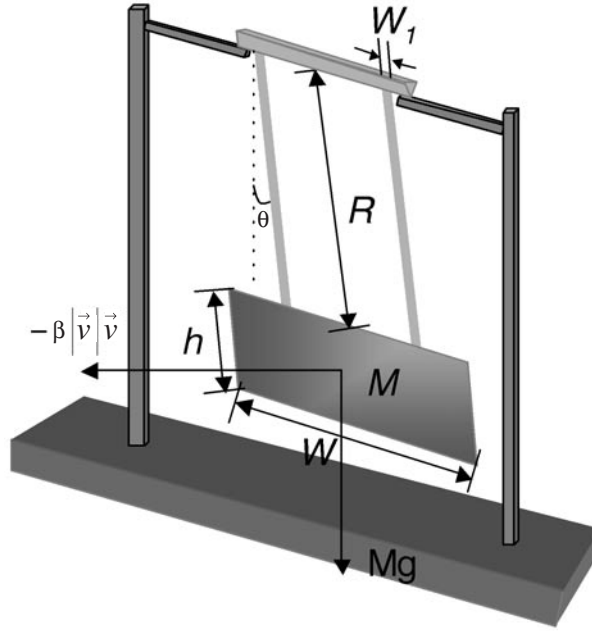
Figure 6. Schematic diagram of a pendulum where air resistance dominates the damping. The pendulum is made of plastic with two strips and a large-area sail at the bottom. Additional mass may be added if greater restoring torque is required. Further tests of the theory can be provided by attaching additional mass and testing the predicted motion with the same damping factors as determined in an initial case.

The value of the moment of inertia, I, is given by

$$I = \frac{1}{3}m_1 R^2 + m_2[(R + h/2) + h^2/12] = \frac{2}{3}\frac{W_1 R}{S}MR^2 + \frac{Wh}{S}M[(R + h/2)^2 + h^2/12]. \quad (21)$$

The restoring torque is

$$\tau_r = -\left[\frac{2}{3}\frac{W_1 R}{S}M\left(\frac{R}{2}\right) + \frac{Wh}{S}M(R + h/2)\right]g\sin\theta. \quad (22)$$

The frictional resistance in the suspension of the pendulum is made small by supporting the rigid object by a knife-edge pivot. At relatively low velocities the friction due to air resistance is $F_f = -a\vec{v} - (c/2)(Wh)\rho_{air}|\vec{v}|\vec{v}$, [2–6] where a is a constant of proportionality, c the drag coefficient, Wh the area of the sail and ρ_{air} the density of air.[2] The coefficients of the two velocity-dependent terms are such that the quadratic term dominates for objects with dimensions that are as large as a few centimetres, unless the speed is extremely low. In the case of an oscillatory motion, such as the pendulum under consideration here, most of the damping occurs when the speed is great enough for the quadratic term to totally dominate. The linear term is only important for relatively tiny objects moving with velocities of a few mm s^{-1} (as with the micrometre-sized oil drops in the Millikan oil drop experiment to determine the

---

[2] The drag force on a sizeable sphere (with a not too small speed) is $\vec{F}_f = -(C_d/2)\rho_{air}A|\vec{v}|\vec{v}$, with $C_d = 0.5$, for velocities well below the range where the transition to turbulent flow occurs. A lucid discussion for the case where the sphere is a baseball can be found in [5]. For a baseball the above expression is valid for any practical situation where $v < 40$ mph ($\sim$18 m s^{-1}). Thus, for our pendulum problem this representation of friction due to motion through air should be very accurate.
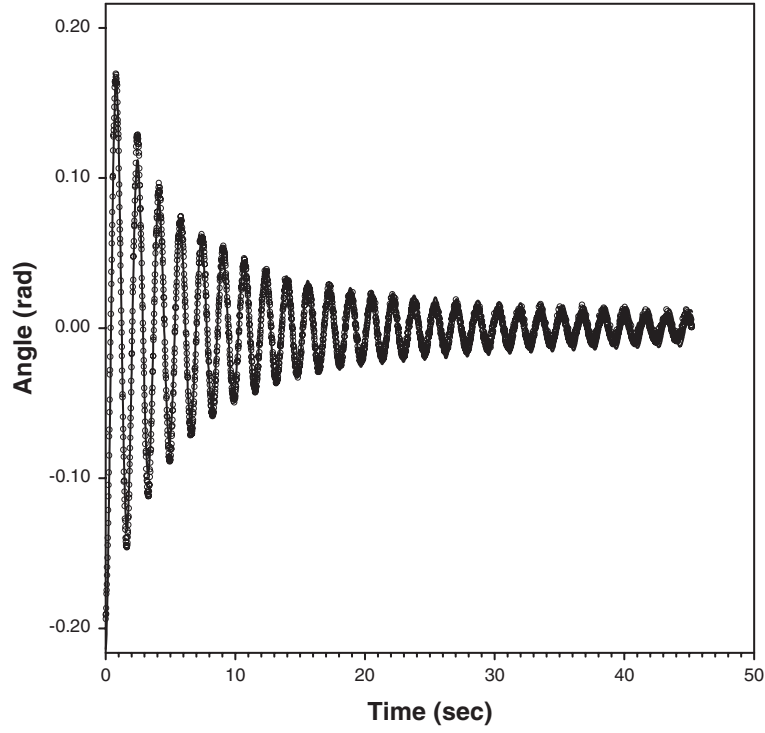
Figure 7. Measured results (circles) as a function of time compared with a curve fit (full curve) with a pendulum damped by air resistance.

charge of the electron). Thus, neglecting the first term, we can write the frictional torque as follows

$$\tau_f = -\frac{c}{2}\rho_{air}(Wh)(R+h/2)|\vec{v}|\vec{v} = -\frac{c}{2}\rho_{air}(Wh)(R+h/2)^3\left|\frac{d\theta}{dt}\right|\frac{d\theta}{dt}. \quad (23)$$

As with the previous cases, we make use of $I d^2\theta/dt^2 = \tau_r + \tau_f$, i.e.

$$\frac{d^2\theta}{dt^2} + \beta\left|\frac{d\theta}{dt}\right|\frac{d\theta}{dt} + \omega^2\theta = 0 \quad (24)$$

where $\beta = \frac{c}{2}\frac{(Wh)\rho_{air}(R+h/2)^2}{I}$ and $\omega^2 = \frac{g}{I}\left(\frac{WR}{S}M(R/2) + \frac{Wh}{S}M(R+h/2)\right)$. Comparing equation (24) with (1) and use the results of equations (9) and (10), we have the case $n = 2$, $I_n = 2/3$ and

$$\frac{dA}{dt} = -\frac{4\beta\omega}{3\pi}A^2 \quad (25)$$

or

$$A = \frac{\theta_0}{1 + (4\beta\omega\theta_0 t/3\pi)} \quad (26)$$

$$\theta = \frac{\theta_0}{1 + (4\beta\omega\theta_0 t/3\pi)}\cos(\omega t + \alpha). \quad (27)$$

Figure 7 shows the experimental results (circles) and the theoretical prediction (full curve). A good agreement between the measured data and theoretical fitting is observed at the beginning. As time increases, a little deviation occurs in the phase, suggesting that the

quadratic resistance is no longer the dominant damping term at lower velocities. The danger of another form of friction starting to dominate for small amplitudes is always present.

In summary, we have demonstrated the experiments of oscillatory motion with three damping mechanisms. We have derived a generalized solution for the damping with constant, linear, quadratic and higher-order velocity dependence. Experimental observation and theoretical calculation agree very well.

References

[1] Robson J 1967 *Basic Tables in Physics* (New York: McGraw-Hill) p 250
[2] Fowles G R and Cassiday G L 1999 *Analytical Mechanics* 6th edn (Orlando, FL: Saunders College Publishing)
[3] Symon K 1971 *Mechanics* 3rd edn (Reading, MA: Addison-Wesley)
[4] Rossberg K 1983 *A First Course in Analytical Mechanics* (New York: Wiley)
[5] Adair R K 1995 The physics of baseball *Phys. Today* **48** 26–31
[6] Frohlich C 1984 *Am. J. Phys.* **52** 325. This paper lists many other references to the literature on air friction.